

# Interface Modification on TiO<sub>2</sub> Electrode Using Dendrimers in Dye-Sensitized Solar Cells

Toshio Nakashima, Norifusa Satoh, Ken Albrecht, and Kimihisa Yamamoto\*

Department of Chemistry, Faculty of Science and Technology, Keio University,  
Yokohama 223-8522, Japan

Received November 16, 2007. Revised Manuscript Received February 3, 2008

The interface modification of dye-sensitized solar cells (DSSCs) in order to remove I<sub>3</sub><sup>−</sup> on the TiO<sub>2</sub> electrodes is important for improving their performance. The suppression of the back electron transfer by a modified interface improves the open-circuit voltage. In this study, we demonstrated that the suppression mechanism using phenylazomethine dendrimers with a triarylamine core (TPA-DPAs) and two other dendrimers, which are a carbazole dendrimer containing a cyclic phenylazomethine of the third generation (CPA-Cz G3) and a half-dendritic phenylazomethine of the fifth generation (Half-DPA G5). Removing I<sub>3</sub><sup>−</sup> and producing I<sup>−</sup> on the TiO<sub>2</sub> electrode by complexation is critical for the suppression of the back electron transfer and promoting the regeneration of the dye in dendrimers having an inner space. Additionally, the presence of various metal compounds in the dendrimers decreased the resistance of the DSSCs, improving fill factor and energy conversion efficiency. We studied that the dendrimer property is changed by the quantitative metal complexation. The fill factor and energy conversion efficiency of the DSSCs are maximized with 0.5 equiv. of SnCl<sub>2</sub> in the TPA-DPAs.

## Introduction

Dye-sensitized solar cells (DSSCs), developed by Grätzel et al., are expected to be an energy resource,<sup>1,2</sup> which are low-cost, flexible,<sup>3</sup> and high-performance cells.<sup>4</sup> However, the efficiency and endurance are still not sufficient; therefore, many researchers are trying to improve the cell performance, such as the open-circuit voltage (*V*<sub>oc</sub>), short circuit current density (*J*<sub>sc</sub>), and fill factor (*ff*).<sup>5</sup> *J*<sub>sc</sub> depends on the characteristics of the dye, such as the light absorption, electron injection efficiency, and adsorption affinities on the TiO<sub>2</sub>. *V*<sub>oc</sub> is restricted by the back electron transfer from the conduction band on the TiO<sub>2</sub> electrode to I<sub>3</sub><sup>−</sup> in the electrolyte.<sup>6</sup> *ff* is influenced by *V*<sub>oc</sub> and the resistance of the cell.

The interface between the semiconductor and electrolyte is important for the cell performance at which the photoin-

duced primary reaction occurs. The modification of the interface has been investigated in order to suppress the back electron transfer. For example, Durrant et al. reported the slow charge recombination using Al<sub>2</sub>O<sub>3</sub>-coated nanoporous TiO<sub>2</sub> films.<sup>7</sup> Because the retardation of the interfacial charge recombination decreases the back electron transfer, the *V*<sub>oc</sub> was improved by 45 mV. Grätzel et al. suggested a series of amphiphilic ruthenium dyes with varying alkyl chain lengths on the TiO<sub>2</sub> electrode.<sup>8</sup> The increase in the dye alkyl chain length results in a slower charge recombination and improvement in *V*<sub>oc</sub>. However, the slower recombination also reduces the rate of the electron injection into the TiO<sub>2</sub> or the dye regeneration by the electrolyte. The C<sub>13</sub> alkyl chain provides the highest performance, but an even longer chain decreases the *J*<sub>sc</sub>. Therefore, the optimization of the interfacial charge transfer by modifying the interface is critical for improvement of the DSSCs.

Recently, we reported the improvement of *V*<sub>oc</sub> using a dendritic phenylazomethine with a triphenylamine core (TPA-DPA).<sup>9</sup> The core of the TPA-DPAs has a redox property and a hole-transporting ability. The dendron has imine units complexed with a Lewis acid, with metal compounds assembled inside. The dendron consists of successive layers of phenylazomethines, causing potential gradients as a result of the difference in the basicity of the imine with the next layer. Thus, the stepwise radial metal assembly occurs within the DPA derivatives. The hydrody-

- (1) (a) Oregan, B.; Grätzel, M. *Nature* **1991**, 353, 737. (b) Palomares, E.; Chifford, J. N.; Haque, S. A.; Lutz, T.; Durrant, J. R. *J. Am. Chem. Soc.* **2003**, 125, 475. (c) Adachi, M.; Murata, Y.; Takao, J.; Sakamoto, M.; Wang, F. *J. Am. Chem. Soc.* **2004**, 126, 14943. (d) Horiuchi, T.; Miura, H.; Sumioka, K.; Uchida, S. *J. Am. Chem. Soc.* **2004**, 126, 12218.
- (2) (a) Nazeeruddin, M. K.; Kay, A.; Rodicio, I.; Humphry-Baker, R.; Miller, E.; Liska, P.; Vlachopoulos, N.; Grätzel, M. *J. Am. Chem. Soc.* **1993**, 115, 6382. (b) Nazeeruddin, M. K.; Pechy, P.; Renouard, T.; Zakeeruddin, S. M.; Humphry-Baker, R.; Cimit, P.; Liska, P.; Cevey, L.; Costa, E.; Shklover, V.; Spiccia, L.; Deacon, G. B.; Bignozzi, C. A.; Grätzel, M. *J. Am. Chem. Soc.* **2001**, 123, 1613.
- (3) Miyasaka, T.; Kijitori, Y.; Ikegami, M. *Electrochemistry* **2007**, 75, 2.
- (4) (a) Nazeeruddin, M. K.; Angelis, F. D.; Fantacci, S.; Selloni, A.; Viscardi, G.; Liska, P.; Ito, S.; Bessho, T.; Grätzel, H. *J. Am. Chem. Soc.* **2005**, 127, 16835. (b) Chiba, Y.; Islam, A.; Watanabe, Y.; Komiyama, R.; Koide, N.; Han, L. *Jpn. J. Appl. Phys.* **2006**, 45, L638.
- (5) Grätzel, M. *J. Photochem. Photobiol., A* **2004**, 164, 3.
- (6) (a) Ferber, J.; Stangl, R.; Luther, J. *Sol. Energy Mater. Sol. Cells* **1998**, 53, 29. (b) He, J.; Benko, G.; Korodi, F.; Polivka, T.; Lomoth, R.; Akemark, B.; Sun, L.; Hagfeldt, A.; Sundström, V. *J. Am. Chem. Soc.* **2002**, 124, 4922. (c) Kusama, H.; Konishi, Y.; Sugihara, H.; Arakawa, H. *Sol. Energy Mater. Cells* **2003**, 80, 167.

- (7) Palomares, E.; Clifford, J. N.; Haque, S. A.; Lutz, T.; Durrant, J. R. *Chem. Commun.* **2002**, 1464.
- (8) Krieze, J. E.; Hirata, N.; Koops, S.; Nazeeruddin, M. K.; Schmidt-Mende, L.; Grätzel, M.; Durrant, J. R. *J. Am. Chem. Soc.* **2006**, 128, 16376.
- (9) Satoh, N.; Nakashima, T.; Yamamoto, K. *J. Am. Chem. Soc.* **2005**, 127, 13030.

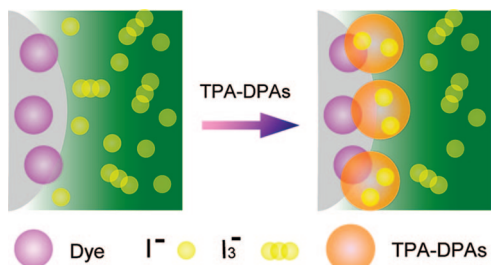


Figure 1. Interface modification by dendrimers on TiO<sub>2</sub> electrode.

nanic radii of the TPA-DPAs linearly increased with the generation number because of their  $\pi$ -conjugated rigid structures.

The interface modification by the TPA-DPAs linearly increased the  $V_{oc}$  with the generation number by about 130 mV at the fifth generation (G5). The suppression of the back electron transfer seems to be caused by two factors. The first factor is the electron transfer kinetics within the TPA-DPAs. The redox active core of the TPA-DPA can reduce the photo-oxidized dye by the electron transfer with the attenuation factor ( $\beta$ ) of 0.35 using electric mixing with the  $\pi$ -conjugated dendron units.<sup>10,11</sup> The back electron transfer, absence of the orbital mixing, possesses the attenuation factor of about 1.6.<sup>12</sup> The difference in the attenuation factors dramatically suppresses the back electron transfer rate in an exponent with the generation growth of the TPA-DPAs. The second factor is the decrease in the concentration of  $I_3^-$ , an electron acceptor of the back electron transfer. The decrease results from the complexation of  $I_3^-$  with the imine ligands of the TPA-DPAs. This complexation is stimulated by the increase in the basicity with the generation number. The increase in the generation number enhances both factors of the electron transfer distance and the association property with  $I_3^-$ , so that we have been unable to perform a precisely controlled experiment (Figure 1).

In this paper, we report the physical characteristics of two other different dendrimers and the DSSC performances using their dendrimers as the controls and then discuss how the interface modification by the dendrimers, having controlled properties such as the hole-transporting, size, shape, and complexation, influences the performance of the DSSCs. The first type of dendrimer is the third generation dendrimer, mainly consisting of hole-transporting carbazole branches and a cyclic phenylazomethine as the core (CPA-Cz G3).<sup>13</sup> Generally, a prominent hole-transfer material possesses a high energy LUMO that acts as an electron blocking layer in organic light emitting diodes, which indicates the possibility of suppressing the back electron transfer. The second type of dendrimer is the Half-DPA G5, a branch unit of TPA-DPA G5, which is expected to be equivalent in basicity (Figure 2).

Additionally, we report the effect on the  $ff$  in the DSSCs by the variety and equivalent of the metal compounds assembled into the TPA-DPAs. The assembly of 1 equiv. of  $SnCl_2$  improves the  $ff$  in the DSSC using the dendrimer, which suggests a decrease in the resistance of the dendrimer. If the redox of the metal compounds assists the hole transfer in the dendrimer, the redox potential and equivalent metal compounds could be an important factor for the  $ff$ . We selected various metal compounds that are complexable with imines, such as  $Sm^{3+}$ ,  $Eu^{3+}$ ,  $Ga^{3+}$ ,  $V^{3+}$ ,  $Sn^{2+}$ ,  $Fe^{3+}$ , and  $Au^{3+}$ .<sup>14</sup> The potentials of  $Sm^{3+}$  and  $Eu^{3+}$  are over the conduction level of TiO<sub>2</sub>. In contrast, the potentials of  $Fe^{3+}$  and  $Au^{3+}$  are under that of the redox couple of  $I^-/I_3^-$ .

## Experimental Section

**Materials.** 4,4'-Diaminodiphenylmethane was purchased from the Tokyo Kasei Kogyo Co. (TCI). Tin(II) chloride was obtained from Wako Pure Chemical Industries. Iron(III) chloride was purchased from Merck, and gallium(III) chloride and vanadium(III) chloride were purchased from Sigma-Aldrich. For fabrication of the DSSCs, Ti-nanoxide T, the N719 dye, and DMPII were obtained from Solaronix. 3-Methoxypropionitrile, tetra-*n*-butyl ammonium triiodide, titanium(IV) chloride, europium(III) trifluoromethanesulfonate, and samarium(III) trifluoromethanesulfonate were purchased from Aldrich. A fluorine-doped tin oxide (FTO) glass sheet was obtained from the Asahi Glass Co. All other chemicals were purchased from Kanto Kagaku. TPA-DPA G5, CPA-Cz G3, and the DPA dendron G5 were synthesized by previous reported methods.<sup>15</sup>

**Analytical Measurement.** The NMR spectra were recorded using a JEOL JMN400 FT-NMR spectrometer (400 MHz) in a  $CDCl_3$  (with tetramethylsilane as the internal standard) solution. The matrix assisted laser desorption/ionization (MALDI) time-of-flight (TOF) mass spectra were obtained using a Shimadzu/Kratos KOMPACT MALDI mass spectrometer (positive mode; Matrix, Dithranol). The analytical size-exclusion chromatography (SEC) was performed using an HPLC (Shimadzu, LC-10AP) equipped with TSK-GEL CMHXL (Tosoh) at 40 °C. Tetrahydrofuran (THF) was used as the eluent at the flow rate of 1 mL/min. The detection was connected to a triple detector (Viscotek, TriSEC model 302). A 100  $\mu$ L aliquot of the THF solution of the Half-DPAs and CPA-Czs (4–5 mg/1 mL) was injected into the gel column.

The UV-vis spectra were measured using a Shimadzu UV-3100PC spectrophotometer. For observation of the titration, a capped quartz cell was filled with 3 mL of a dehydrated chloroform/ acetonitrile ( $v/v = 1/1$ ) solution containing the Half-DPA G5 (2.5  $\mu$ M). The measurement of the spectra and addition of the  $SnCl_2$  or  $FeCl_3$  solution continued until the spectral change was saturated. The depth profiles were analyzed by the glow discharge optical emission spectroscopy (GDOES (Horiba Co., GD profiler2)). The photocurrent, photovoltage, and  $I-V$  curves were measured using an  $I-V$  tracer (Eiko Seiki Co., MP-160) under irradiation by simulated solar light (Eiko Seiki Co., ESS200, AM1.5G, 100 mW/cm<sup>2</sup>).

**Fabrication of DSSCs.** The DSSCs using the dendrimers were fabricated by a previous method.<sup>15</sup> For the photocurrent measurements, a sandwich-type open electrochemical cell was used which

- (10) (a) Helms, A.; Heiler, D.; McLendon, G. *J. Am. Chem. Soc.* **1992**, *114*, 6227. (b) Tour, J. M. *Chem. Rev.* **1996**, *96*, 537.
- (11) Davis, W. D.; Svec, W. A.; Ratner, M. A.; Wasielewski, M. R. *Nature* **1998**, *396*, 60.
- (12) Hirata, N.; Lagref, J. J.; Palomares, F. J.; Durrant, J. R.; Nazeeruddin, M. K.; Grätzel, M.; Censo, D. D. *Chem. Eur. J.* **2004**, *10*, 595.
- (13) Kimoto, A.; Cho, J. S.; Higuchi, M.; Yamamoto, K. *Macromol. Symp.* **2004**, *51*, 209.

- (14) Takanashi, K.; Fujii, A.; Nakajima, R.; Chiba, H.; Higuchi, M.; Einaga, Y.; Yamamoto, K. *Bull. Chem. Soc. Jpn.* **2007**, *80*, 1563.
- (15) (a) Higuchi, M.; Shiki, S.; Yamamoto, K. *Org. Lett.* **2000**, *2*, 3079. (b) Takanashi, K.; Chiba, H.; Higuchi, M.; Yamamoto, K. *Org. Lett.* **2004**, *6*, 1709.

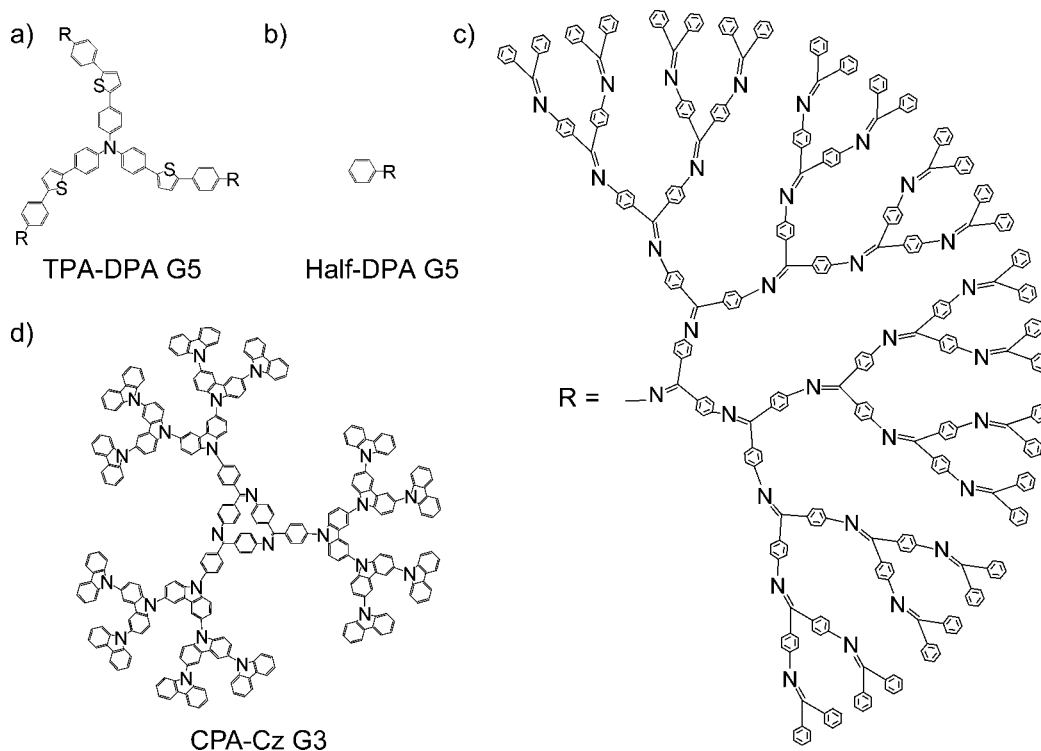


**Figure 2.** Structure of the dendrimers. (a) Triphenylamine core (TPA-DPA G5). (b) Half-dendritic phenylazomethine core (Half-DPA G5). (c) Generation 5 of DPA dendron units. (d) Carbazole dendrimer containing cyclic phenylazomethine of generation 3 (CPA-Cz G3).

is composed of a dye-adsorbed TiO<sub>2</sub> electrode, a spacer, and a Pt counter electrode. To prepare a TiO<sub>2</sub> electrode, the TiO<sub>2</sub> paste (Ti-Nanoxide T) was deposited onto a FTO glass (fluorine-doped SnO<sub>2</sub>) and then heated under air for 10 min at 450 °C. The thickness was approximately 10 μm. The electrode was soaked overnight in a mixture solution of N719 dye. Dendrimers were spin-cast on the dye-adsorbed TiO<sub>2</sub> electrode. The dye-coated semiconductor film was illuminated through a conducting glass support with a mask. The active electrode area was 0.16 cm<sup>2</sup>.

**Synthesis of Half-DPA G5.** To a mixture of the DPA dendron G5 (127 mg, 0.022 mmol), aniline (0.04 mL, 0.39 mmol), DABCO (100 mg, 0.89 mmol), and chlorobenzene (20 mL), warmed at 80 °C, was added titanium(IV) chloride (0.06 mmol) under a nitrogen atmosphere. The reaction mixture was warmed at 125 °C and stirred for 1 h. The precipitate was then filtered off, the filtrate was evaporated, and the residue was purified by preparative SEC to produce the Half-DPA G5 as a yellow powder (105 mg, 83%); <sup>1</sup>H NMR (400 Hz, CDCl<sub>3</sub>, 25 °C, TMS) δ = 7.74–6.43 (m, 285H); <sup>13</sup>C NMR (400 Hz, CDCl<sub>3</sub>, 25 °C, TMS) δ = 169.00, 168.75, 168.48, 168.17, 167.91, 167.77, 154.16, 153.92, 153.75, 152.24, 151.93, 139.32, 139.11, 135.77, 135.62, 134.27, 131.73, 130.90, 130.62, 130.11, 129.88, 129.39, 128.83, 128.63, 128.19, 128.03, 127.88, 127.41, 121.63, 121.30, 120.85, 120.50, 120.28, 120.28, 120.02, 119.76; MS (MALDI-TOF) *m/z* 5631.1 (M<sup>+</sup>), calcd 5633.85. Anal. Calcd for C<sub>409</sub>H<sub>285</sub>N<sub>31</sub>: C, 87.19; H, 5.10; N, 7.71%. Found: C, 86.66; H, 5.129; N, 7.613.

## Results and Discussion

**Size and Structure of Dendrimers.** The sizes and forms of the macromolecule can be analyzed by a triple-detected SEC, having viscometry, laser light scattering, and refractive index (RI) detection capabilities.<sup>16,17</sup> The hydrodynamic radii

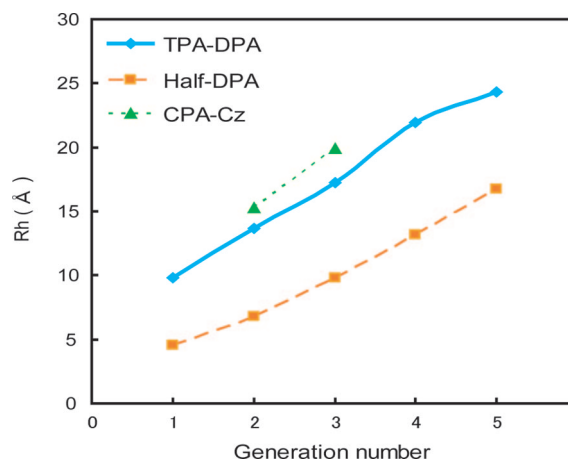


**Figure 3.** Hydrodynamic radii as a function of generation number in TPA-DPA, CPA-Cz, and Half-DPA.

linearly increased with the generation number. The measured radii of CPA-Cz G3 and Half-DPA-G5 were 2.00 nm and 1.66 nm, which are comparable to TPA-DPA G4 (2.11 nm) and G3 (1.69 nm), respectively (Figure 3).<sup>18</sup>

The relation between the molecular weight *M* and intrinsic viscosity  $[\eta]$  is described by the Mark–Houwink Sakurada equation as follows:

$$[\eta] = KM^a$$

In the Mark–Houwink Sakurada plot ( $\log M$  vs  $\log[\eta]$ ), the constant *a* is changed because of the form of the

(16) Satoh, N.; Cho, J.-S.; Higuchi, M.; Yamamoto, K. *J. Am. Chem. Soc.* **2003**, *125*, 8104.

(17) Yamamoto, K.; Higuchi, M.; Kimoto, A.; Imaoka, T.; Masachika, K. *Bull. Chem. Soc. Jpn.* **2005**, *78*, 349.

(18) (a) Ihre, H.; Hult, A.; Soderlind, H. *J. Am. Chem. Soc.* **1996**, *118*, 6388. (b) Cardona, C. M.; Kaifer, A. E. *J. Am. Chem. Soc.* **1998**, *120*, 4023.



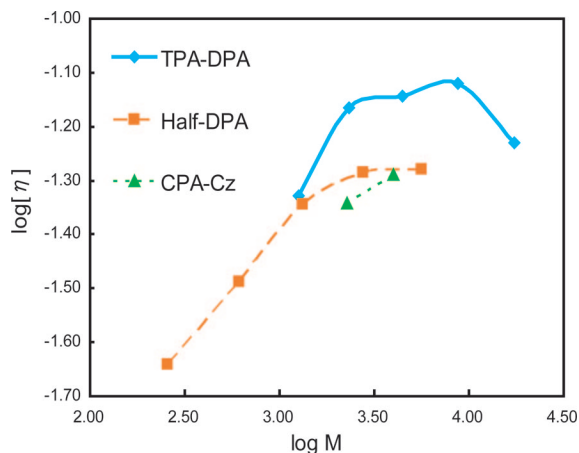


**Figure 4.** Mark-Houwink Sakurada plots of TPA-DPA, CPA-Cz, and Half-DPA.

macromolecule. As an example,  $a = 2$  for a rod shape,  $a = 0.7$  for a random coil, and  $a = 0$  for a spherical shape. The constant  $a$  in the large generation of TPA-DPA and Half-DPA is close to 0, indicating that these dendrimers have a rigid spherical structure. That of CPA-Cz is 0.21, suggesting that CPA-Cz, as well as the other one, also have a nearly spherical structure. The larger dendrimer would reach the spherical structure. These results indicate that the dendrimers have a higher density than the linear polymers. The constant  $K$  indicates the density of the polymers. In TPA-DPA G $n$  ( $n = 1-4$ ), the density is lower than the Half-DPAs and CPA-Cz, because TPA-DPA has a larger core. While CPA-Cz has the highest density, CPA-Cz is expected to have a greater shell effect due to the high density in the polymers (Figure 4).

**Complexation Properties of Dendrimers.** CPA-Cz G3 mainly consists of phenylcarbazole, having only three azomethine units.<sup>19</sup> The complexation of phenylcarbazole (PCz) and tetra-*n*-butylammonium triiodide was investigated by the Job plot and <sup>1</sup>H NMR (Supporting Information, S1). No changes were observed in the absorbance and chemical shift of the PCz, indicating no interaction between the PCz and I<sub>3</sub><sup>−</sup>.

In contrast, the Half-DPA G5 showed a complexation ability similar to TPA-DPA G5. The complexation of Half-DPA G5 was evaluated by titration with SnCl<sub>2</sub> (Figure 5).<sup>20</sup> The addition of SnCl<sub>2</sub> to the solution of the Half-DPA G5 resulted in a color change from yellow to orange that was attributed to the complexation. Using UV-vis spectroscopy to monitor the titration until an equimolar amount of SnCl<sub>2</sub> was added, we observed four changes in the position of the isosbestic point. The isosbestic points appeared at 369, 367, 366, and 365 nm upon the addition of 0–1, 2–3, 4–15, and 16–31 equiv. of SnCl<sub>2</sub>, respectively. The added equivalent to shift the isosbestic points is coincident with the number of imines in each layer, although 12 equiv. for the isosbestic point at 366 nm matched the sum of the imines in the third

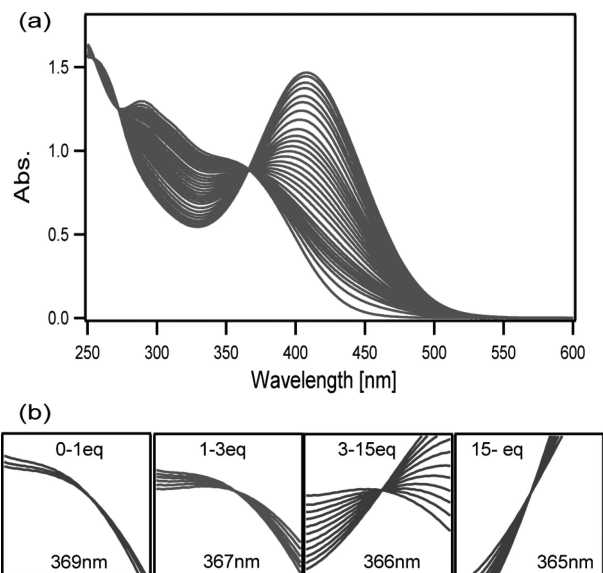


**Figure 5.** Stepwise radial complexation of SnCl<sub>2</sub> into Half-DPA G5. (a) UV-vis spectral change. (b) Enlargements showing isosbestic points during complexation with SnCl<sub>2</sub>.

**Table 1. Performance of DSSCs Using CPA-Cz G3**

treatment	$J_{sc}$ (mA/cm <sup>2</sup> )	$V_{oc}$ (mV)	$ff$	$eff$ (%)
none	15.8	659	0.56	5.8
CPA-Cz G3	15.3	660	0.56	5.7

and fourth layers. This behavior suggests that the stepwise complexation proceeded except for the complexation to the third and fourth layers. The random complexation to the third and fourth layers would result from the small difference in basicity between the third and the fourth layers. This complexation behavior is quite similar to that of TPA-DPA G5, indicating that the basicity of the Half-DPA G5 is comparable to that in TPA-DPA G5. On the other hand, FeCl<sub>3</sub> strongly complexes with the imine units. By titration with FeCl<sub>3</sub>, five isosbestic points appear, indicating the difference in the basicity between the third and fourth layers is small but exists (Supporting Information, S2).

**Characteristic Performance of DSSCs Using Two Dendrimers.** The DSSCs using CPA-Cz G3, a  $\pi$ -conjugated dendrimer with the high hole-transporting property but little complexation ability, contrary to our expectation, showed no difference in performance to a blank cell (Table 1). No improvement in the  $V_{oc}$  would result from the lack of complexation with I<sub>3</sub><sup>−</sup>. In the case of the SAMs of the alkyl chains and the coat of metal oxides, these highly packed structures effectively remove I<sub>3</sub><sup>−</sup> from the TiO<sub>2</sub> surface. Although dendrimers have the most highly packed structures in polymers, small molecules, like I<sub>3</sub><sup>−</sup>, can be captured inside the structures.<sup>21</sup> As a result of the presence of I<sub>3</sub><sup>−</sup> in the dendrimers, the distance between the TiO<sub>2</sub> conduction bands and I<sub>3</sub><sup>−</sup> would not be absent.

The importance of the complexation is also indicated by the time dependence of the energy efficiency of a DSSC using TPA-DPA G5. We fabricated a closed cell using TPA-DPA G5 for the first time to discuss the time dependency. It took 5 h to reach the maximum point in the energy

(19) CPA-Cz G $n$  ( $n = 1-3$ ) have the ability to complex with Sn<sup>2+</sup> and Eu<sup>3+</sup> with little difference in their generation, suggesting a dendrimer with a low density interior; ref 13.

(20) (a) Yamamoto, K.; Higuchi, M.; Shiki, S.; Tsuruta, M.; Chiba, H. *Nature* **2002**, 415, 509. (b) Imaoka, T.; Horiguchi, H.; Yamamoto, K. *J. Am. Chem. Soc.* **2003**, 125, 340. (c) Enoki, O.; Katoh, H.; Yamamoto, K. *Org. Lett.* **2006**, 8, 569.

(21) Jansen, J. F.; G, A.; de Brabander-van den Berg, E. M. M.; Meijer, E. W. *Science* **1994**, 266, 1226.

**Table 2.** Performance of DSSCs Using Half-DPA G5 and TPA-DPA G5

	$J_{sc}$ (mA/cm <sup>2</sup> )	$V_{oc}$ (mV)	$ff$	$eff$ (%)
none	14.9	634	0.47	4.4
DPA-H G5	14.4	692	0.53	5.3
Half-TPA-DPA G5	14.7	720	0.54	5.8

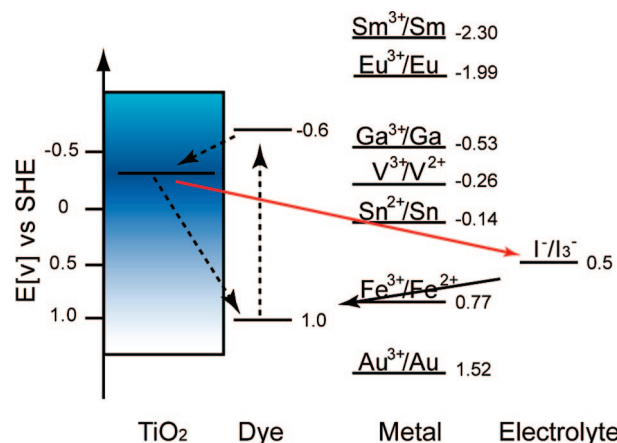
**Table 3.** Performance of DSSCs Using TPA-DPA G4 Complexed with 1 equiv. of Sm<sup>3+</sup>, Eu<sup>3+</sup>, Ga<sup>3+</sup>, V<sup>3+</sup>, Fe<sup>3+</sup>, and Au<sup>3+</sup>

dendrimer	$J_{sc}$ (mA/cm <sup>2</sup> )	$V_{oc}$ (mV)	$ff$	$eff$ (%)
none	13.6	729	0.53	5.2
G4	12.1	795	0.61	5.9
Sm(OTf) <sub>3</sub> @G4	12.4	818	0.56	5.3
Eu(OTf) <sub>3</sub> @G4	12.1	793	0.55	5.7
none	15.2	723	0.55	6.1
G4	14.3	826	0.53	6.5
GaCl <sub>3</sub> @G4	14.9	836	0.57	7.1
none	15.2	708	0.57	6.2
G4	14.4	773	0.57	6.5
VCl <sub>3</sub> @G4	14.4	779	0.62	7.0
none	12.9	716	0.53	5.0
G4	14.2	765	0.50	5.4
FeCl <sub>3</sub> @G4	13.6	779	0.55	5.8
none	15.0	730	0.54	5.9
G4	14.3	804	0.57	6.6
AuCl <sub>3</sub> @G4	13.4	817	0.62	6.8

conversion efficiency (Supporting Information, S3), which agrees with the time to finish the complexation reaction of the imine ligand and I<sub>3</sub><sup>−</sup> (Supporting Information, S4). This fact supports the importance of the complexation in dendrimers.

The comparison of the DSSCs using TPA-DPA G5 and Half-DPA G5 enables us to discuss the influence of the size and the structure of the dendrimers in the DSSCs, because of the same complexation ability (Table 2). Although both cells improved the  $V_{oc}$  and efficiency ( $eff$ ) over the blank cells, the improvement of TPA-DPA G5 is superior to the Half-DPA G5 regarding  $J_{sc}$  and  $V_{oc}$ . Because the weight amount of the cast dendrimers was the same, this result indicates the necessity to construct a larger structure under the same condition of basicity and amount of ligands on the surface. On the other hand, the cell performance using the Half-DPA G5 is superior to the previous data using TPA-DPA G3, having a lower basicity and the same hydrodynamic radius as the Half-DPA G5. This fact supports the importance of stronger ligands in the dendrimers.

The casting of TPA-DPAs on a TiO<sub>2</sub> electrode had a similar effect on other materials, such as the self-assembled monolayers (SAMs) of the alkyl chain and Al<sub>2</sub>O<sub>3</sub> coating. Removing I<sub>3</sub><sup>−</sup> from the interface of TiO<sub>2</sub> is important for the suppression of the back electron transfer. Polymers having a complexation property are not only for removing I<sub>3</sub><sup>−</sup> from the TiO<sub>2</sub> electrode but also for generating I<sup>−</sup> from I<sub>3</sub><sup>−</sup>, and it is easy to handle. Although other materials decrease the injection into TiO<sub>2</sub> or the regeneration of the dye, the complexable dendrimers do not decrease it due to the generated I<sup>−</sup> from the complexed with I<sub>3</sub><sup>−</sup>. Additionally, the  $\pi$ -conjugated polymers have a small  $\beta$  for the electron transfer from the TiO<sub>2</sub> conduction band to the electrolyte and a large  $\beta$  for that from the electrolyte to the dye. At the interface of the TiO<sub>2</sub> electrode, the concentration of I<sup>−</sup> increases, while that of I<sub>3</sub><sup>−</sup> decreases. Therefore, the com-

**Figure 6.** Energy diagram of the modeled DSSC and redox levels of metal compounds (Sm<sup>3+</sup>, Eu<sup>3+</sup>, Ga<sup>3+</sup>, V<sup>3+</sup>, Sn<sup>2+</sup>, Fe<sup>3+</sup>, Au<sup>3+</sup>).**Table 4.** Performance of DSSCs Using TPA-DPA G4 Complexed with 0.3 equiv. of Sm<sup>3+</sup> and Eu<sup>3+</sup>

dendrimer	$J_{sc}$ (mA/cm <sup>2</sup> )	$V_{oc}$ (mV)	$ff$	$eff$ (%)
none	13.6	724	0.56	5.6
G4	14.2	784	0.58	6.5
Sm(OTf) <sub>3</sub>	14.0	795	0.60	6.8
Eu(OTf) <sub>3</sub>	14.5	808	0.58	6.7

plexable and  $\pi$ -conjugated dendritic polymers do not decrease the injection into the TiO<sub>2</sub> electrode and  $J_{sc}$  is comparable with the other materials. Since a more optimistic and design of the dendritic polymers is possible, the casting of polymers in the DSSCs would be potentially better than the other materials.

**Metal-Effect Assembling in the DSSCs.** The cell performances using TPA-DPA G4 complexed with an equivalent amount of various metal compounds, such as Sm<sup>3+</sup>, Eu<sup>3+</sup>, Ga<sup>3+</sup>, V<sup>3+</sup>, Sn<sup>2+</sup>, Fe<sup>3+</sup>, and Au<sup>3+</sup>, are summarized in Table 3. All cells using the dendrimer complexes increased 0.05 points in  $ff$  except for the Sm<sup>3+</sup> and Eu<sup>3+</sup> complexes. The redox potentials of Ga<sup>3+</sup>, V<sup>3+</sup>, Sn<sup>2+</sup>, Fe<sup>3+</sup>, and Au<sup>3+</sup> are −0.53, −0.26, −0.14, 0.77, and 1.52 V versus SHE, respectively (Figure 6).<sup>22</sup> The difference in the redox potential does not affect the cell performances; therefore, the redox of these additives would not be related to the electron transporting mechanism in the dendrimers. The difference between the effective group, Ga<sup>3+</sup>, V<sup>3+</sup>, Sn<sup>2+</sup>, Fe<sup>3+</sup>, and Au<sup>3+</sup>, and the ineffective group, Sm<sup>3+</sup> and Eu<sup>3+</sup>, is the coordination number with the imine ligands. Although the complexation number of the effective group is 1, that of the ineffective group is 3. The decrease in the complexation equivalent from 1 equiv. to 0.3 equiv. results in the improved  $ff$  in the DSSCs using the Sm<sup>3+</sup> and Eu<sup>3+</sup> complexes (Table 4). These results suggest that not the kind of added metal but the amount of the metal complexed with the imines would be important.

The effect of the complexation was examined using TPA-DPA G3 and G4 in the range of 0.2, 0.5, 1, 3, and 5 equiv. of SnCl<sub>2</sub> (Figure 7, Table 5). The maximum  $ff$  and  $eff$  were observed at 0.5 equiv. of SnCl<sub>2</sub> in both the TPA-DPA G3 and the TPA-DPA G4. The increase in the  $ff$  indicates a

(22) Bard, A. J.; Parsons, R.; Jordan, J., Eds. *Standard Potentials in Aqueous Solution*; Marcel Dekker: New York, 1985.

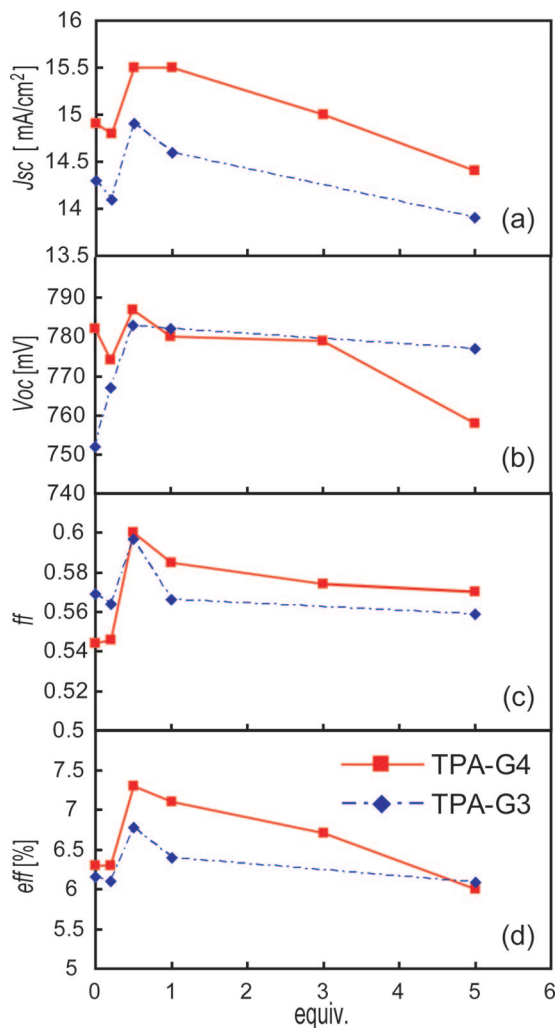


**Figure 7.** Variation in (a) short-current density  $J_{sc}$ , (b) open-circuit voltage  $V_{oc}$ , (c) fill factor  $ff$ , and (d) energy conversion efficiency  $eff$  with the ratio of  $\text{SnCl}_2$ /TPA-DPA G4.

**Table 5.** Performance of DSSCs Using TPA-DPA G3 and G4 in the Range of 0, 0.2, 0.5, 1, 3, and 5 equiv. of  $\text{SnCl}_2$  (G3/G4)

equiv	$J_{sc}$ (mA/cm <sup>2</sup> )	$V_{oc}$ (mV)	$ff$	$eff$ (%)
0	14.3/14.9	752/782	0.57/0.54	6.1/6.3
0.2	14.1/14.8	767/774	0.56/0.55	6.1/6.3
0.5	14.9/15.5	783/787	0.60/0.60	6.8/7.3
1	14.6/15.5	782/780	0.57/0.59	6.4/7.1
3	—/15.0	—/779	—/0.57	—/6.7
5	13.9/14.4	777/758	0.56/0.57	6.1/6.0

decrease in the resistance of the DSSCs and that of the dendrimers. However, the added excess equivalent of  $\text{SnCl}_2$  decreases  $J_{sc}$  and  $ff$ , because of promoting the back electron transfer.<sup>22</sup> Not the weight percent but the equivalent of  $\text{SnCl}_2$  added to the dendrimer affects the cell performances, which suggests that a  $\text{SnCl}_2$  complexes with a dendrimer and influences only one  $\pi$ -conjugated molecular chain. These phenomena are also observed in an organic light emitting diode (OLED) using DPA derivatives as the hole-transporting layer.<sup>23</sup>

## Conclusion

For the suppression of the back electron transfer using a polymer, it is a very important factor to remove  $\text{I}_3^-$  from the surface of the  $\text{TiO}_2$  electrode. This is also observed in the DSSCs using dendrimers with a high density and compact structure. We propose an advantage that affects the displacement of the equilibrium to  $\text{I}^-$  by the complexation in order to remove  $\text{I}_3^-$  inside the polymers. Thus, the dendrimers do not retard the desired electron transfer, differing from the SAMs of the alkyl chain and  $\text{Al}_2\text{O}_3$  coating. The dendrimers would play a role similar to an intrinsic layer as a charge separating layer in amorphous silicon solar cells.

For the same complexation ability, the larger distance between the  $\text{TiO}_2$  electrode and electrolyte shows the higher performances in the DSSCs. TPA-DPA G6 and the larger dendrimers, expected to have a stronger complexation ability and larger structure, may contribute to the higher performances. However, the synthesis would be impossible because of the steric barrier.<sup>9</sup>

Generally, the decreased connection on the interface of the DSSCs decreases  $V_{oc}$ . Therefore, casting the dendrimers with the high molecular weight in the  $\text{TiO}_2$  electrode decreases the  $V_{oc}$ . A polymer with a high viscosity and large structure is difficult to penetrate the nanopores on the  $\text{TiO}_2$  electrode, thus decreasing the connection. Since the dendrimers with the monodispersed molecular weight have compact structure, it is easy for them to penetrate into nanoporous  $\text{TiO}_2$  electrode.<sup>24,25</sup>

In order to examine the effect of the  $\pi$ -conjugated structure, it is important to know how non- $\pi$ -conjugated dendrimer with the same complexation ability affects the performances in the DSSCs. Their dendrimers, however, may not be present on the  $\text{TiO}_2$  electrode, because of dissolving to the electrolyte.

The addition of the metal compounds into the dendrimers showed an effect like doping, resulting in the easy electron transfer, although the kind of metal compounds did not change and the equivalent of the complexed imines improved the  $ff$ . The  $ff$  and  $eff$  of the DSSCs were maximized with 0.5 equiv. of  $\text{SnCl}_2$  in the TPA-DPAs.

**Acknowledgment.** This study was supported in part by the Core Research for Evolutional Science and Technology (CREST) program of the Japan Science and Technology (JST) Agency and by Grants-in-Aid for the Scientific Research (Nos. 19205020, 19750120) from the Ministry of Education, Culture, Sports, Science and Technology (MEXT) of Japan.

**Supporting Information Available:** Additional data (PDF). This material is available free of charge via the Internet at <http://pubs.acs.org>.

CM703279U

(23) (a) Cho, J.-S.; Kimoto, A.; Higuchi, M.; Yamamoto, K. *Macromol. Chem. Phys.* **2005**, *206*, 635. (b) Satoh, N.; Cho, J.-S.; Higuchi, M.; Yamamoto, K. *J. Photopolym. Sci. Technol.* **2005**, *18*, 55.

(24) Higuchi, M.; Shiki, S.; Ariga, K.; Yamamoto, K. *J. Am. Chem. Soc.* **2001**, *123*, 4414.

(25) Dendrimers have been reported to construct a packing structure on a substrate in ref 24. The dendrimer membrane is beautifully formed in the direction of the plane. Dendrimers disperse into the  $\text{TiO}_2$  electrode by the glow discharge optical emission spectroscopy (S5; GDOES). The amount of C element of dendrimer origin might be little. However, dendrimers cannot insert a smaller nanoporous  $\text{TiO}_2$  electrode than the dendrimer diameter (ca. 4.4 nm).